European Cells and Materials Vol. 39 2020 (pages 77-95) DOI: 10.22203/eCM.v039a05 ISSN 1473-2262

REVISITING THE "RACE FOR THE SURFACE" IN A PRE-CLINICAL MODEL OF IMPLANT INFECTION

S.M. Shiels*, L.H. Mangum and J.C. Wenke

U.S. Army Institute of Surgical Research, Orthopaedic Trauma Department, Fort Sam Houston, TX, USA

Abstract

Orthopaedic implant use increases infection risk. Implant infection risk can be explained by the "race for the surface" concept, where there is competition between host-cell integration and bacterial colonisation. Although generally accepted, the temporal dynamics have not been elucidated *in vivo*. Using a bilateral intramedullary rat model, *Staphylococcus aureus* was injected into the tail vein either immediately after or 1, 3 and 7 d following implant placement. This allowed assessment of the temporal interplay between bacterial colonisation and host-cell adhesion by uncoupling implant placement and bacterial challenge. 2 weeks following inoculation, animals were anaesthetised, euthanised and implants and tissues harvested for bacterial enumeration. To assess host participation in implant protection, additional animals were not inoculated but euthanised at 1, 3 or 7 d and the host cells adhered to the implant were evaluated by flow cytometry and microscopy. As time between implant placement and bacterial challenge increased, infection rate and bioburden decreased. All implants had measurable bioburden when challenged at day 1, but only two implants had recoverable bacteria when inoculated 7 d after implant placement. This protection against infection corresponded to a shift in host cell population surrounding the implant. Initially, cells present were primarily non-differentiated stem cells, such as bone marrow mesenchymal stem cells, or immature haematopoietic cells. At day 7, there was a mature monocyte/macrophage population. The present study illustrated a direct relationship between host immune cell attachment and decrease in bacterial colonisation, providing guidance for antimicrobial release devices to protect orthopaedic implants against bacterial colonisation.

Keywords: *Staphylococcus aureus*, implant colonisation, orthopaedic, haematogenous, intramedullary nail, peri-prosthetic joint infection.

***Address for correspondence**: S.M. Shiels, 3698 Chambers Pass, Fort Sam Houston, TX 78234, USA.
Telephone number: +1 2105393654 Email: stefanie.m.shiels.ctr@mail.mil

Introduction

Although often necessary for treatment, orthopaedic implant use increases the risk of infection (Zimmerli and Sendi, 2011). Bacteria rapidly colonise the surface of implanted biomaterials, resulting in recalcitrant biofilm formation (Elek and Conen, 1957; Gristina, 1987; Mayberry-Carson *et al.*, 1984). A key to implant survival is for host-tissue integration to occur prior to bacterial attachment (Gristina, 1987; Gristina *et al.*, 1988). Host integration involves an intimate bond between host cells and the implant surface, which is promoted by the implant's biocompatibility and its encouragement for a normal immune response after implant placement. Persistence of an implant-centred infection can result in elongated hospital stay with subsequent surgeries, implant removal and exchange or even limb amputation (Zimmerli and Sendi, 2011). A common anti-infective approach is to prevent bacterial attachment by surface modifications (Campoccia *et al.*, 2013). Techniques for preventing bacterial colonisation include modifications and surface coatings that can prevent attachment or eradicate local bacteria (Shiels *et al.*, 2018a). Unfortunately, the types of modifications that can be utilised are generally limited due to local tissue response, *in situ* coating degradation or antibiotic-release exhaustion (Campoccia *et al.*, 2013).

With more than 2,000 citations to the seminal article, the concept of "race for the surface" is widely accepted as the theory that best explains the competition between host and bacteria for implant colonisation (Gristina, 1987). If the implant is colonised by bacteria first, recalcitrant bacterial biofilms form, contributing to device failure and further treatment (Costerton, 2005). Conversely, host-tissue integration with the implant occurring before bacterial colonisation reduces the risk of

infection, increases implant survival and improves patient recovery (Subbiahdoss *et al.*, 2009). Although this concept has been well elucidated using *in vitro* techniques, there are few *in vivo* experiments demonstrating the relationship between implant placement and bacterial colonisation (Busscher *et al.*, 2012; Martinez-Perez *et al.*, 2017; Perez-Tanoira *et al.*, 2017; Subbiahdoss *et al.*, 2011). Rabbit models have been used to identify the likelihood of prosthetic infection using a haematogenous route of administration (Blomgren and Lindgren, 1981; Southwood *et al.*, 1985). Similarly, using a rodent model of haematogenous implant infection, the implant placement and bacterial challenge can be uncoupled in an effort to better understand the early time course relationship between host-cell attachment and bacterial colonisation. This information will provide valuable guidance to design effective strategies to reduce implant-related infections.

Materials and Methods

Experimental overview

To thoroughly investigate the temporal relationship between implant placement and exposure to bacteria, two experiments were performed. Part I uncoupled implant placement from the bacterial challenge, providing an insight on how long it takes for the host to protect the implant against bacterial colonisation. Part II determined the cell population on and immediately around the biomaterial at various time points after implantation to elucidate what host cells are potentially playing a protective role.

Animal research was conducted in compliance with the Animal Welfare Act, the implementing Animal Welfare Regulations and the principles of the Guide for the Care and Use of Laboratory Animals, National Research Council. The Institutional Animal Care and Use Committee of the US Army Institute of Surgical Research approved all research conducted. The facility where the research was conducted is fully accredited by the Association for Assessment and Accreditation of Laboratory Animal Care (AAALAC).

Animals were observed daily for at least the first 3 d after both surgery and bacterial inoculation for signs of pain and distress such as lethargy, lack of grooming, lack of mobility and weight loss. If there were indications of a failure to thrive, such as no response upon provocation or weight loss more than 20 %, the animal was immediately anaesthetised, euthanised and excluded from the study. If animals were found dead in their cage, they were excluded from the study.

Part I: evaluating bacterial colonisation

UAMS-1 (ATCC49230), a wild-type parental strain of an osteomyelitis isolate of methicillin-susceptible *Staphylococcus aureus* (*S. aureus*) was used as pathogen (Gillaspy *et al.*, 1995). UAMS-1 is both clinically relevant and has been used extensively in orthopaedic research (An and Freidman, 1998; Ellington *et al.*, 2006; Shiels *et al.*, 2018b; Smeltzer *et al.*, 1997). This will be referred to as UAMS-1P. Although known reference strains and subtypes could have been used for the present study, reporter variants of UAMS-1P were investigated. Strain variations impact infection rate, biofilm formation and recalcitrance to infection (Jenkins *et al.*, 2015; Recker *et al.*, 2017). Although fluorescent or luminescent reporter strains are commonly interchanged with parental strains to improve visualisation, measurement and reduce animal numbers, they, similarly to strain variations, have differences in virulence and biofilm-forming capacities as compared to their parental strain (Knodler *et al.*, 2005; Margolin, 2000; Southward and Surette, 2002; Suff and Waddington, 2017). Green fluorescent protein (GFP) UAMS-1 (UAMS-1GFP) contains a GFP plasmid introduced by phage transduction (acquired from the Dental Trauma Research Department of the U.S. Army Institute of Surgical Research) (Chen *et al.*, 2012). Luminescent UAMS-1 (UAMS-1LUM) contains a stable copy of the *Photorhabdus luminescens lux* operon on its bacterial chromosome (Xen40, PerkinElmer). Previous unpublished experience with these reporters indicated differences in colonisation and virulence. To better understand host-cell attachment, bacterial colonisation relationship with regards to biofilm and virulence while minimising the differences between the bacteria, these modified UAM-1 pathogens were also included.

An *in vivo* model of haematogenous implant infection was used to evaluate the effect time has on implant colonisation of UAMS-1 (Shiels *et al.*, 2015). Titanium Kirschner wire implants (1.25 mm × 23 mm, Synthes), which are used to model intramedullary nails (IMNs), were inserted in a retrograde fashion in the intramedullary canal of both femora of anaesthetised male Sprague-Dawley rats (N = 72, 364 ± 1 g; n = 6/group) (Fig. 1). Briefly, a medial incision was made through the skin and into the joint capsule. The patella was reflexed laterally, exposing the intercondylar notch. An 18G bevelled, cannulated needle was used to access and ream the intramedullary canal through the intercondylar notch. The IMN was pushed into the canal, flush with the tibial plateau and arthrotomy and skin were closed. Following surgical closure, animals were randomly separated into one of three bacteria groups (UAMS-1P, UAMS-1GFP or UAMS-1LUM) then into one of the four time-to-inoculation groups [immediately post-operatively or post-operative day (POD) 1, 3 or 7; Fig. 1]. Bacteria [$1.3 \times 10^7 \pm 5.2 \times 10^5$ colony forming units (CFU)/300 μL] were previously prepared in tryptic soy broth (TSB, Thermo Fisher Scientific) and frozen during log-phase growth. On the day of surgery, the bacteria were thawed, washed, suspended in saline and injected into the tail vein. 2 weeks following inoculation, animals were anaesthetised, euthanised with an overdose of sodium pentobarbital and hind limbs were

Table 1. *S. aureus* genes of interest. F = forward, R = reverse. * both used as housekeeping genes..

Gene		Sequence	Description
agrA	F	AAC TGC ACA TAC ACG CTT ACA	Required for high-level post-exponential phase expression of a series of secreted proteins. Involved in virulence potential (Traber *et al.*, 2008).
	R	GGC AAT GAG TCT GTG AGA TTT (Kalinka *et al.*, 2014)	
icaA	F	CTT GCT GGC GCA GTC AAT AC	A member of a gene series that encodes proteins mediating the synthesis of polysaccharide intercellular adhesion and polysaccharide/adhesion in staphylococci species for biofilm formation (Yazdani *et al.*, 2006).
	R	GTA GCC AAC GTC GAC AAC TG (Iqbal *et al.*, 2016)	
rnaIII	F	AAT TAG CAA GTG AGT AAC ATT TGC TAG T	Known to regulate the expression of many *S. aureus* genes encoding exoproteins and cell-wall-associated proteins. In *S. aureus*, RNAIII acts as the effector of the *agr* quorum sensing system and is transcribed from the P3 operon (Traber *et al.*, 2008). RNAIII also encodes for the toxin delta-hemolysin (Verdon *et al.*, 2009).
	R	GAT GTT GTT TAC GAT AGC TTA CAT GC (Sully *et al.*, 2014)	
sarA	F	GTA ATG AGC ATG ATG AAA GAA CTG T	Global regulator, with both positive and negative effects, that controls the expression of several virulence factors and the biofilm formation process in a cell-density-dependent manner. Required for transcription of the primary transcripts RNAII and RNAIII generated by *agr* locus. Negatively regulates the expression of *spa* (protein A) and *aur* (metalloprotease aureolysin) (Valle *et al.*, 2003).
	R	CGT TGT TTG CTT CAG TGA TTC G (Iqbal *et al.*, 2016)	
*aroE**	F	CTA TCC ACT TGC CAT CTT TTA T	Housekeeping gene
	R	ATG GCT TTA ATA TCA CAA TTC C	
*gyrB**	F	AAT TGA AGC AGG CTA TGT GT	Housekeeping gene
	R	ATA GAC CAT TTT GGT GTT GG	

aseptically harvested. Samples were processed for bacterial enumeration. IMNs were placed into sterile saline and sonicated to remove attached bacteria. Femora were snap-frozen, pulverised to a fine powder, resuspended in sterile saline and vortexed to collect bacteria. Serial dilutions of IMN and bone supernatants were plated on to sheep's blood agar and incubated overnight. CFU were counted and normalised to sample weight.

Bacterial growth: in vitro

To measure growth rate *in vitro*, the three variations of UAMS-1 were grown in TSB overnight. Dilutions of optical density 0.05, as measured at 600 nm (OD600), were prepared from the overnight cultures in TSB and grown at 37 °C. Optical density measurements were taken over a 24 h period to measure the change in absorbance and, thus, in bacteria number. Three samples per bacteria variation were prepared and measured.

Bacterial biofilm production: in vitro

UAMS-1P, UAMS-1GFP and UAMS-1LUM were grown in TSB at 37 °C to OD600 0.12. Glass chamber slides were prepared by precoating each well with 10 % human serum. Bacteria in TSB were added to each well and incubated for 24 h at 37 °C to form a biofilm. Subsequently, bacterial biofilms were stained with Filmtracer LIVE/DEAD biofilm viability stain (Invitrogen). Images were acquired with a 488 nm laser using the Fluoview 1000 (Olympus) confocal laser scanning microscope at 20× magnification. Biomass and biofilm thickness were calculated by Comstat 2 analysis software (Heydorn *et al.*, 2000; Vorregaard M (2008) Comstat2-a modern 3D image analysis environment for biofilms. Technical University of Denmark, Lyngby, Denmark.) using 2D Z-stack imaging of 4.17 μm-thick sections to prepare 3D biofilm structures from the different biofilms. One biofilm per variation was prepared and 10 random measurements acquired per biofilm.

Transcription of bacterial virulence and biofilm genes: in vitro

To determine the role of virulence in the risk of infection, RNA was recovered and analysed using real-time PCR from UAMS-1P, UAMS-1GFP and UAMS-1LUM. First, bacteria were grown to OD600

0.25 in three conditions: TSB medium at 37 °C, TSB medium plus 10 % human serum at 37 °C and TSB medium at 37 °C then frozen at − 80 °C. Bacteria were collected by centrifugation, resuspended in RNAprotect (Qiagen) and incubated for 10 min at room temperature. Cells were collected by centrifugation, resuspended in lysing reagent (1 mg/mL lysostaphin, 1000 U/μL lysozyme and 600 mU/mL Proteinase K), vortexed and incubated for 15 min at 37 °C with intermittent vortexing. Following incubation, Buffer RLT (Qiagen) substituted with β-mercaptoethanol was added to the lysing bacteria, transferred to a tube with 0.5 mm glass beads and homogenised (Bead Ruptor Elite, Omni International, Kennesaw, GA, USA). RNA was collected from the lysed bacteria cells using the EZ1 (Qiagen) and, after concentration was determined (Nanodrop, Thermo Fisher Scientific) and integrity checked (TapeStation, Agilent) (Busscher *et al.*, 2012), frozen. Genomic DNA, cDNA and real-time PCR were prepared according to the RT2 qPCR Primer Assay Handbook using the RT2 SYBER Green Mastermix and the CFX 96 Thermocycler (Biorad). Genes of interest were *agrA, icaA, rnaiii* and *sarA* (Table 1) (Iqbal *et al.*, 2016; Kalinka *et al.*, 2014; Sully *et al.*, 2014; Traber *et al.*, 2008; Valle *et al.*, 2003; Verdon *et al.*, 2009; Yazdani *et al.*, 2006). One stock of each bacterial strain was prepared and RNA recovered. Three replicates of each stock were processed for RT2 qPCR.

Part II: quantitative analysis of host-cell-implant interaction

The "race for the surface" involves bacteria competing against host cells. A model mimicking the infection study was chosen to identify the cellular host components involved in implant integration prior to a bacterial challenge. Similarly to part I, IMNs were inserted in femora of anaesthetised Sprague Dawley rats (N = 18, male, 425 ± 9 g; n = 6 animals/group; 3 limbs/outcome measure) as previously described. Following surgical closure, animals were randomly assigned to one of three time-point groups, POD 1, 3 or 7 (Fig. 1). On the day of tissue collection, animals were anaesthetised, euthanised with an overdose of pentobarbital and hind limbs aseptically harvested. The host-cell population on the IMN and within the bone marrow (BM) was evaluated by flow cytometry, histology and scanning electron microscopy (SEM).

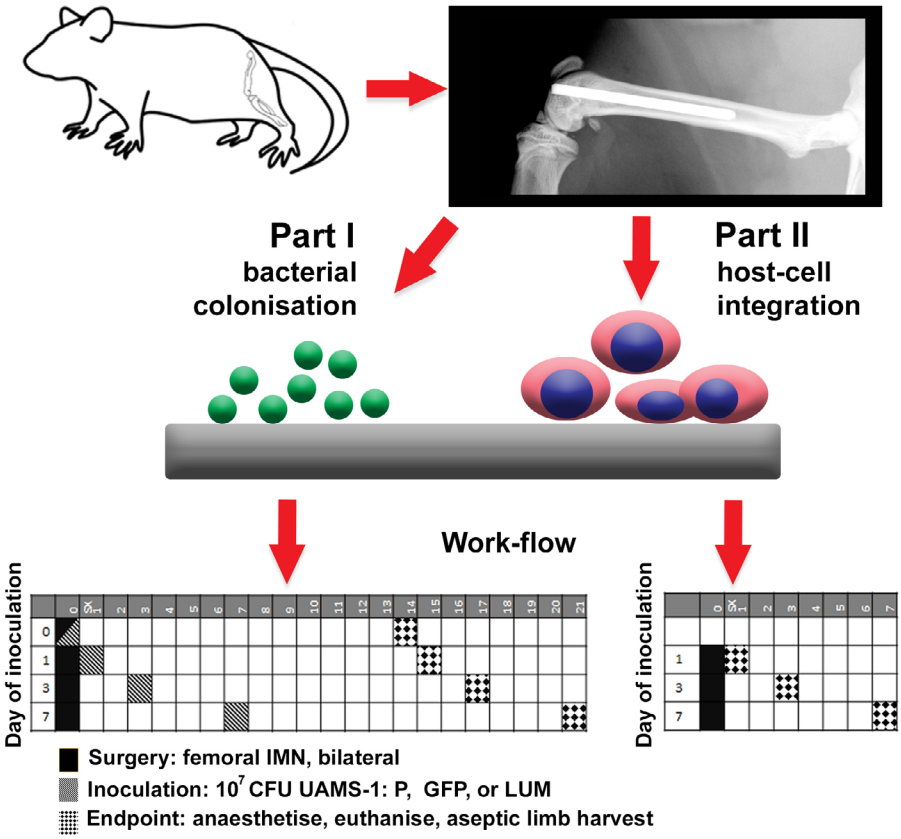

Fig. 1. Complete study design and workflow of part I and part II. Part I assessed bacterial colonisation of the implants by bacteria from a haematogenous source. Animals received implants on day 0 (black). After being separated into groups, animals were injected through tail vein with *S. aureus* either immediately post-operative or 1, 3 and 7 d later (grey). 14 d after inoculation, animals were anaesthetised, euthanised and implants and tissues harvested for quantitative enumeration (diamonds). Part II assessed host-cell integration of titanium implants using the same time-point used in part I. Animals received implants on day 0 (black). After being separated into groups, animals were anaesthetised, euthanised and implants harvested 1, 3 or 7 d later (diamonds). Implants and tissues were processed for flow cytometry, histology or SEM.

Flow cytometry

At the time of euthanasia, femora were disarticulated, freed from soft-tissue and the proximal third removed with sterile rongeurs. IMNs were removed aseptically and placed into sterile 5 mL flow cytometry tubes containing pre-warmed 0.05 % trypsin-ethylenediaminetetraacetic acid (EDTA) (Life Technologies) and incubated for 3-5 min with gentle warming to detach adherent cells. Next, 10× volumes of sterile, low-endotoxin, 10 % foetal bovine serum (FBS, Gibco) solution prepared in sterile phosphate-buffered saline (PBS; Life Technologies) was added to inactivate the trypsin, then stored on ice. Following removal of the IMN, the femoral canal was flushed using sterile fluorescence-activated cell sorting (FACS)-PBS (Sterile Milentyi AutoMACS Rinsing solution) containing 1 % bovine serum albumin (BSA, Miltenyi Biotec), to collect BM cells.

Following inactivation of trypsin-EDTA with 10 % FBS, IMNs were removed from the tube and placed on a 100 μm cell strainer. Each wire was rinsed with sterile, ice-cold FACS-PBS to remove any weakly attached cells. Following the initial rinse, K-wires were discarded and the remaining cell suspension was filtered through the same 100 μm cell strainers. Bone marrow samples were agitated by pipetting to dissociate aggregates, then filtered using 100 μm cell strainers. Cell suspensions were centrifuged at 400 ×*g* for 5 min at 4 °C and the resulting pellets were treated with 1× red blood cell lysis buffer (Biolegend, San Diego, CA, USA) according to manufacturer's directions. Cell pellets were resuspended and viable cells counted using trypan blue staining solution on a haemocytometer.

Cells were stained with the antibodies CD45-BV510 (Clone: OX-1BD; OptiBuild, San Jose, CA, USA), CD11b-FITC (Clone: OX-42; BD Pharmingen, BD Biosciences), CD90-APC/Cy7 (Clone: OX-7; Biolegend) and CD68-Dylight® 405 (Clone: ED1; Novus Biologicals, Littleton, CO, USA). Briefly, cells from both the K-wire (IMN) and the BM were washed with FACS-PBS and incubated with Fc-block (BD Pharmingen) to prevent non-specific binding. Then, cells were stained in FACS-PBS with surface marker antigens CD11b, CD90 and CD45 for 30 min at 4 °C in the dark. Cells were washed twice, then prepared for intracellular staining using a commercially available buffer set according to the manufacturer's instructions (eBioscience Intracellular Fixation & Permeabilization Buffer Set, Thermo Fisher Scientific). Briefly, cells were fixed with fixation buffer for 30 min at room temperature, then washed twice with permeabilisation buffer. Cells were stained with CD68 in permeabilisation buffer for 30 min at room temperature in the dark, washed twice, then resuspended in 500 μL FACS-PBS prior to analysis using a multi-parameter flow cytometer (FACSMelody, BD Biosciences). Flow cytometric compensation was performed using fluorescent compensation beads (BD Ultracomp, BD Biosciences).

Cellular attachment to the implant surface, as well as changes to inflammatory cell populations in the BM were assessed by FACS at PODs 1, 3 and 7. A gating strategy to remove debris and cells with

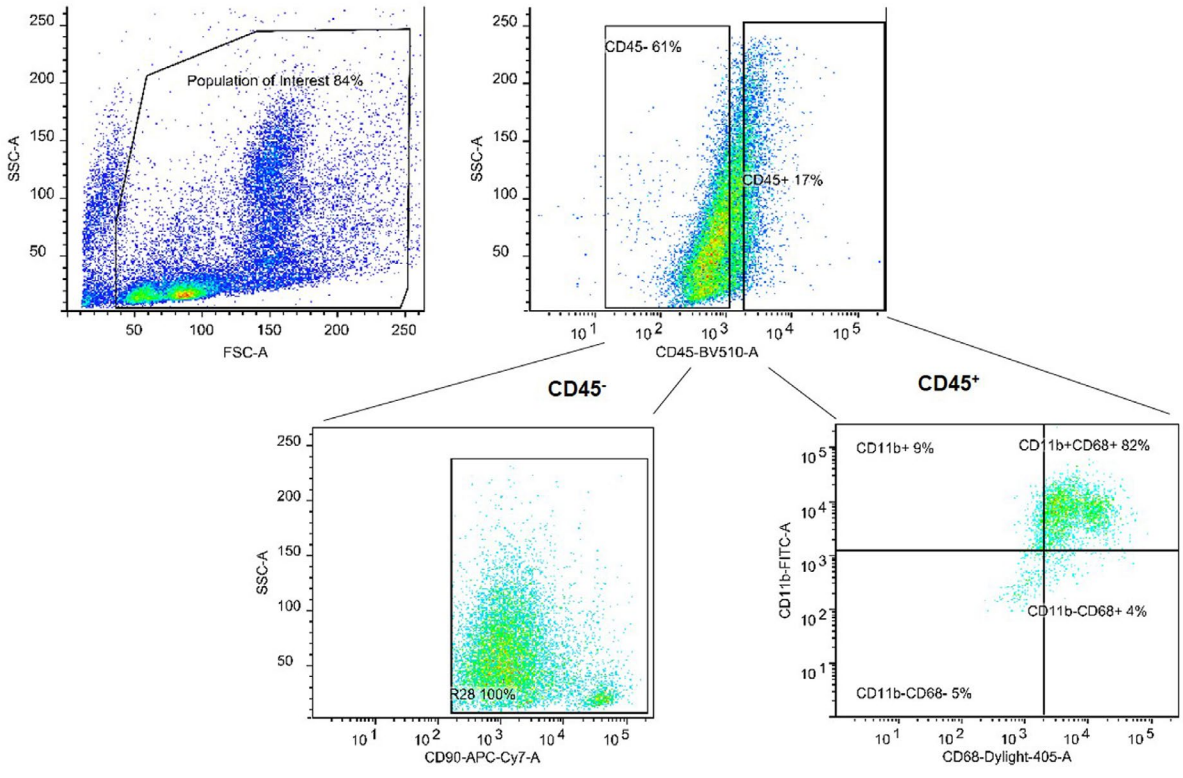

Fig. 2. A broad gating strategy was used to include both high and low SSC populations to include most of the cells in the stromal fraction. Then, cells were gated and analysed based on CD45⁺ or CD45⁻ staining.

higher forward and side scatter, followed by double discrimination, was used to analyse singlet cells (Fig. 2). Cells were separated based on CD45 staining, a pan-haematopoietic marker, then analysed for surface marker expression of CD90, found on stem cells and fibroblasts, or CD11b, which is a monocyte and macrophage marker. $CD45^-$ and $CD11b^+$ cells were further assessed for intracellular expression of CD68, a lysosomal marker that is highly enriched in macrophages but has also been documented in human fibroblasts (Gottfried *et al.*, 2008).

Histology

Following euthanasia, femora were disarticulated, freed from tissue, the proximal third removed and submerged in 10 % phosphate-buffered formalin for 2 weeks without removal of the IMN. Femora were processed for plastic-embedded histology by dehydration in graded ethanol series, clearing in xylene and embedding with polymethylmethacrylate (Tecnovit 1720, Exakt Technologies, Oklahoma City, OK, USA). Cross sections were prepared through the proximal epiphysis and mid-diaphysis by water-cooled band saw (Exakt Technologies), ground and polished to 30 μm thickness. Sections were stained with toluidine blue and basic fuchsin and reviewed for cellular content adjacent to the implant using brightfield microscopy at 100×.

SEM

IMNs were recovered from femora and placed into 3 % glutaraldehyde (Electron Microscopy Sciences, Hatfield, PA, USA) in phosphate buffer (pH 7.4) for 2 h. After 2 h, IMNs were rinsed three times with phosphate buffer followed by serial dehydration steps from 50 to 100 % ethanol. After the final 100 % ethanol step, IMNs were dried for SEM by first placing them in 50 % hexamethydisilazane (HMDS) in ethanol followed by 100 % HMDS. K-wires were left to air dry before storage at room temperature. IMNs were sputter-coated with gold and carbon and imaged on a Zeiss Sigma VP scanning electron microscope.

Data analysis

Data are represented as mean ± standard error of the mean and analysed using ANOVA with an alpha of 0.05, unless otherwise stated. Flow cytometry data are represented as mean ± standard deviation (SD). Infection rate and mortality rate are represented as fraction of the sample or group, respectively. A Fisher's exact test was used to detect differences among the infection rate. GraphPad's Prism and QuickCalcs (GraphPad Software) were used to run these analyses. A linear mixed model was used to analyse the $\log_{10}$(CFU) measured in bone tissue and on the IMN. In each regression model, inoculation day, strain and interaction of these two factors were used as fixed explanatory variables. Animal leg was included as a random effect in the model to account for samples being collected from both femora of each animal. The best fitting residual covariance structure for each outcome was determined using Akaike information criterion (AIC) and Bayesian information

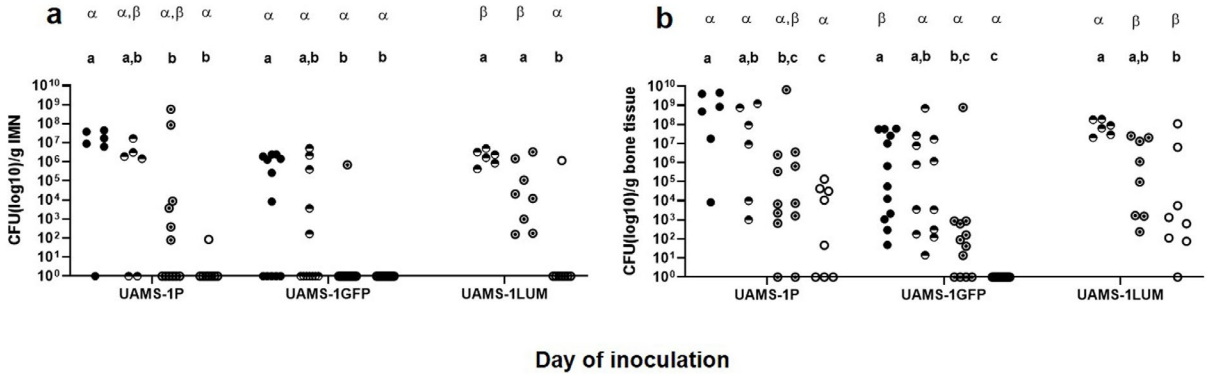

c

Day of inoculation	0	1	3	7
UAMS–1P	5/6	4/6	4/12	0/8
UAMS–1GFP	7/12	4/12	1/12	0/12
UAMS–1LUM	0/0	6/6	5/8	1/8

Fig. 3. Effect of time and reporter on bacterial burden and infection rate in a IMN model. Bacteria on the (**a**) IMN and within the (**b**) bone samples recovered from each animal. Each point represents a separate limb. Latin letters are comparisons of times within each group, UAMS-1P UAMS-1GFP or UAMS-1LUM. Greek letters are comparison of groups within each time. Horizontal line represents group median. Groups that do not share the same Latin letter within each group are different across time ($p < 0.05$). Time points that do not share the same Greek letter are different across groups ($p < 0.05$). (**c**) Infection rate for total number of limbs that completed the study. Animals that did not complete the study were excluded. Infection rate was determined based on the presence of more than 10^3 bacteria in either bone or IMN.

criterion (BIC) statistics, with a compound symmetry structure selected for all models. The *p*-values for all *post-hoc* pairwise comparisons (p_{adj}) were adjusted according to the appropriate method (*i.e.* Tukey-Kramer). The linear mixed model was performed using SAS 9.4 (SAS Institute, Cary, NC, USA) and significance was evaluated using an alpha of 0.05.

Results

Delaying bacterial challenge resulted in less colonisation on the IMN

Post-operative time to bacterial challenge played a significant role in the amount of bioburden and rate of infection. As the time between implant placement and bacterial inoculation increased, the colonisation of the IMN decreased (Fig. 3**a**). When injected immediately after implant placement, the wires were heavily colonised by bacteria. None of the UAMS-1LUM animals inoculated at the time of surgery survived until the end of the study period; two were found dead in their cage and four were euthanised due to failure to thrive. When UAMS-1P and UAMS-1LUM were injected 7 d after surgery, only one wire from each group had recoverable bacteria, 8.5×10^2 and 1.2×10^6 CFU, respectively. With increased time to inoculation, the UAMS-1GFP bioburden on the implant quickly diminished, falling from $8.2 \times 10^5 \pm 3.0 \times 10^5$, when inoculated at the time of surgery, to $5.8 \times 10^4 \pm 5.8 \times 10^4$ by POD 3. No bacteria were recovered when inoculated at POD 7. A similar decreasing trend was identified in the bone tissue (Fig. 3**b**). While UAMS-1P and UAMS-1LUM bone samples were both still infected in 4 of 8 limbs when injected at POD 7, the number of bacteria decreased from when the animals were inoculated 1 d after surgery. Additionally, UAMS-1GFP had no recoverable bacteria from the bone tissue when injected at POD 7. Infection rates decreased as time between incident surgery and bacteria inoculation increased (Fig. 3**c**). Infection was defined quantitatively when samples contained $> 10^3$ CFU/g sample. Infection was supported by gross findings (*i.e.* purulence, osteolysis) and radiographic indications (reactive bone formation, lucency and cortical thinning).

Radiographs acquired at the end of the study supported the quantitative microbiology, revealing severe osteolytic bone, reactive bone formation and lucent bone tissue (Fig. 4). When inoculated at the time of surgery, all groups contained animals that presented with osteolysis around the implantation site and knee. As time from implant placement to inoculation increased, those animals inoculated with UAMS-1GFP presented decreasing radiographic

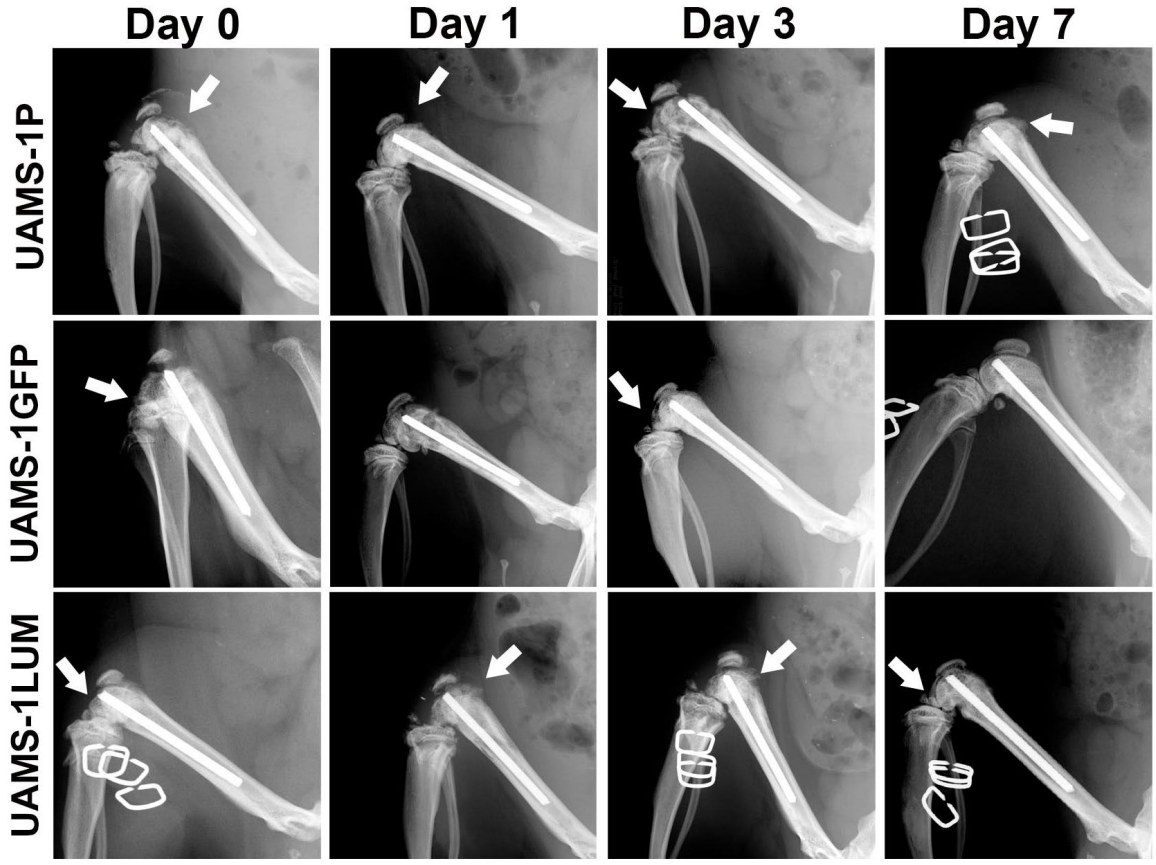

Fig. 4. Representative radiographs 14 d after intravenous inoculation of *S. aureus*. Arrows indicate areas of active bone resorption, periosteal reaction and osteolysis. When injected after 7 d, UAMS-1P and UAMS-1LUM group had signs of osteolysis whereas UAMS-1GFP group did not. Image for UAMS-1LUM day 0 is 2 d post-injection.

signs of infection whereas the number of animals within UAMS-1P and UAMS-1LUM groups with radiographic signs of infection was constant whether inoculated at PODs 0 or 7. UAMS-1GFP animals were the least likely to present radiographic indications of infection, with only ~ 63 % of the animal quantitatively infected, showing osteolysis and lucency in their coordinating radiographs, as compared to 84 and 88 % for UAMS-1P and UAMS-1GFP, respectively.

Animal weight change and mortality was indicative of general animal health and supported the quantitative microbiology. Those animals that received UAMS-1GFP survived the length of the study and were able to regain preoperative weight when inoculated 7 d post surgery (Fig. 5). None of the animals that received UAMS-1P or UAM-1LUM recovered to preoperative weight. As previously mentioned, there was a 6/6 mortality rate of the animals inoculated with UAMS-1LUM when injected at the time of surgery due to failure to thrive. Although survival rate slightly improved as bacterial challenge was delayed, there continued to be deaths within the UAMS-1P and UAMS-1LUM groups whereas the mortality rate for the UAMS-1GFP group was zero (Fig. 5). A board-certified veterinary pathologist determined that septicaemia and shock were the cause of death for several animals, grossly indicated by the rapid weight loss and kidney lesions. Implant-associated findings were not determined from these animals and they were excluded from the study.

Considering the differences observed when animals were inoculated with different reporters, further characterisation into each reporter strain was performed. Using optical density, it was revealed that UAMS-1GFP grew slower than both UAMS-1P and UAMS-1LUM in TSB, which could have implications *in vivo*. Over the first 8 h, UAMS-1GFP had a growth rate of 0.060/h whereas UAMS-1P and UAMS-1LUM had growth rates of 0.092/h and 0.086/h, respectively (Fig. 6). However, by 24 h, UAMS-1GFP had lower growth rate than the UAMS-1P parental strain. When bacterial biofilm formation was evaluated for bioburden, thickness and biomass, there were visual differences in biofilm appearance, with UAMS-1P forming a more uniform biofilm as compared to UAMS-1GFP and UAMS-1LUM, which showed patches of low growth (Fig. 7). Nevertheless, there were no differences in average CFU, biofilm thickness or living biomass, a measurement of the amount of

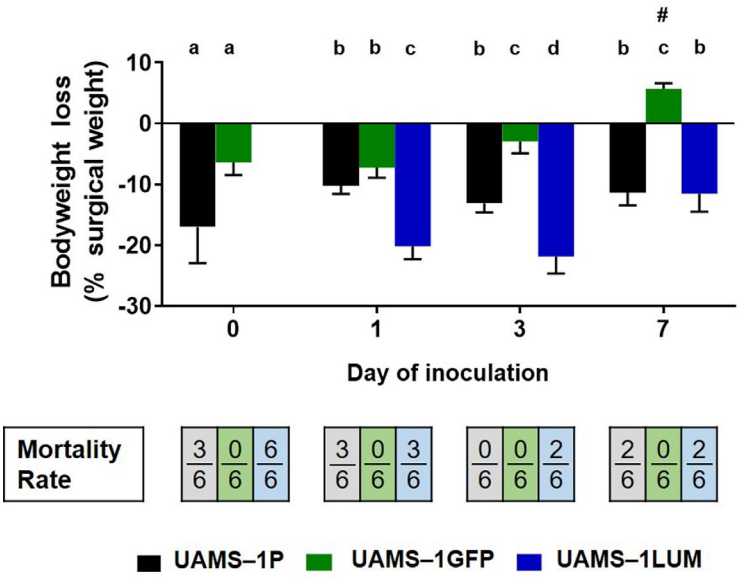

Fig. 5. Average group weight loss and mortality rate. Time points that do not share the same Latin letter within each group are different ($p < 0.05$, ANOVA). # represents significance between groups within each time-point ($p < 0.05$), *t*-test (day 0) or ANOVA (day 1, 3 or 7). There was significant difference in mortality rate between UAMS-1GFP and UAMS-1LUM groups at day 0 inoculation time ($p < 0.01$; Fisher's exact test).

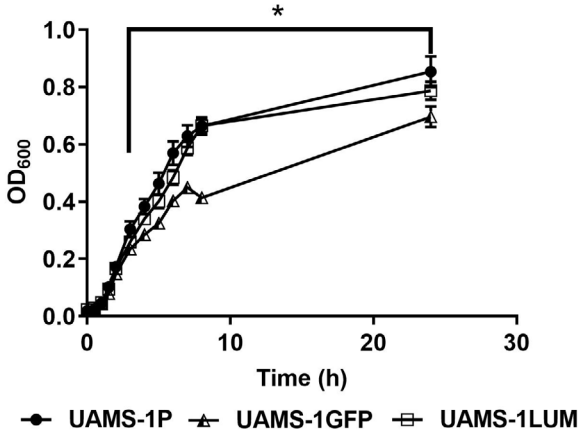

Fig. 6. Bacteria growth curve. There was a significant difference in the growth of UAMS-1GFP as compared to UAMS-1P between 3 and 24 h at each of the measured time points. There was no difference between UAMS-1LUM and UAMS-1P during the growth period except at the 6 h measurement.

biological material present in a given area, among the three bacteria types (Fig. 7). Compared to the parental UAMS-1P type, UAMS-1GFP and UAMS-1LUM expressed different patterns of the important virulence regulator *agrA* and biofilm-associated locus, *icaA*. While UAMS-1GFP had reduced *agrA* expression, its *icaA* expression was 5.4-fold upregulated (Fig. 8). Strangely, *icaA* and *sarA* loci were down-regulated in the UAMS-1GFP when the samples were frozen. Considering their importance in biofilm formation, this may explain the reduced biofilm formation *in vivo*. In contrast, UAMS-1LUM expressed 5.3-fold upregulated virulence regulator *agrA* in all preparation conditions. Understandably, the presence of soluble host factors, quorum sensing and biofilm formation will alter these expressions. These expressions provided a representation of the genetic differences among these reporter strains and some explanation for the mortality rate differences detected during the animal study.

Host-cell interaction with the implant changes over time

A flow cytometry protocol was developed to isolate and analyse the cellular populations that were adherent to the IMN and within the BM at 1, 3 and 7 d post implantation (Fig. 9). The gating strategy implemented was meant to include most of the cells in the stromal fraction (Fig. 2) while minimising doublets, potential debris and cells with very high scatter properties. Then, cells were gated and analysed based on $CD45^+$ or $CD45^-$ staining. Further gating was used to assess cells of monocytic ($CD45^+$/$CD11B^+$/$CD68^+$) or potential mesenchymal lineage ($CD45^-$/$CD90^+$). While not well described in rats, some authors have described a $CD45^-$/$CD68^+$ population of human primary fibroblasts that brightly stain for $CD68^+$ (Gottfried *et al.*, 2008); this population was assessed as well. 1 d following implantation, approximately 44 % of all $CD45^-$ cells on the IMN surface appeared to be of a mesenchymal or fibroblast lineage, exhibiting a $CD45^-$/$CD90^+$ phenotype (Table 2). While the percentage of $CD45^-$ cells did not decrease over time, the number of $CD45^-$/$CD90^+$ cells dropped drastically over the course of 7 d. $CD45^-$/$CD68^+$ cells were transiently increased on the IMN surface at day 3, but this population dropped off by day 7. Conversely, few cells exhibited a monocytic/macrophage phenotype early after implantation of the IMN. At day 1, only 12 % of the $CD45^+$ population co-expressed CD11b and CD68. This percentage increased to approximately one third of all $CD45^+$ cells by day 7. During this time course, the percentage of $CD45^+$ cells did not change dramatically. In the bone marrow, the percentage of $CD45^-$/$CD90^+$ did not vary widely over the course of the experiment. However, the percentage of monocyte/macrophage cells within the $CD45^+$ population increased on day 3 and 7. In comparison to the IMN, populations of $CD45^-$/$CD68^+$ fibroblasts in BM increased at day 3 and remained elevated at day 7.

Histological sections stained with toluidine blue and basic fuchsin supported the cytometric findings (Fig. 10). At day 1, small cells were trapped in a fibrous matrix adjacent to the implant. After 3 d, the separation between haematopoietic and

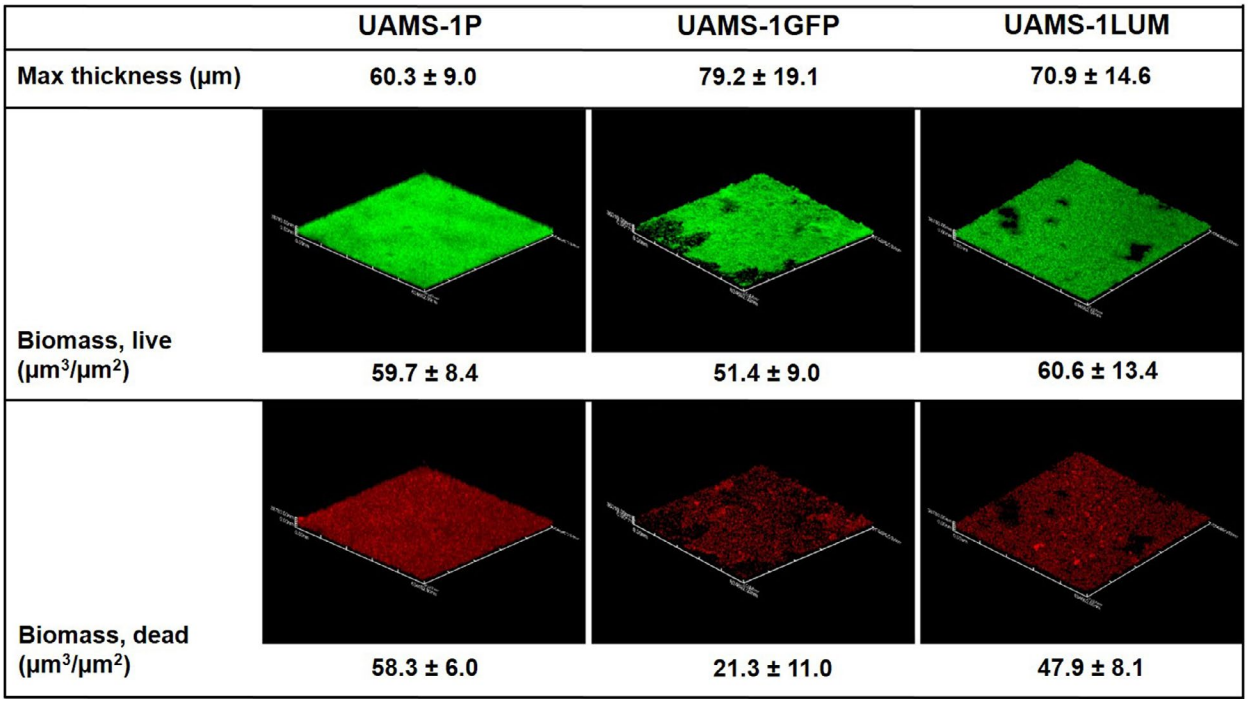

Fig. 7. Bacterial biofilm formation. There were visual differences in biofilm formation between UAMS-1P, UAMS-1GFP and UAMS-1LUM. UAMS-1P grew in a uniform lawn whereas both UAMS-1GFP and UAMS-1LUM had patches of no growth. While there were no differences in live biomass ($p = 0.63$; Kruskal-Wallis), dead biomass of UAMS-1GFP was significantly different from that of UAMS-1P (* $p < 0.05$).

non-haematopoietic cells became visible with the appearance of macrophages and spindle cells. At day 7, there were foreign body giant cell formation, a fusion of macrophages that were indistinguishable with the flow cytometry stains used.

SEM images of the IMN recovered from the bones corroborated the host-cell change on the surface (Fig. 11). When recovered early, after day 1, the IMNs were consistently covered in erythrocytes and spindle cells. As time progressed, the cell population on the IMN shifted to larger macrophage and monocyte-like cells.

Discussion

By uncoupling the initial implant placement from the bacterial challenge, the IMN's susceptibility to bacterial colonisation was determined and linked to the host adhesion in an immunocompetent rat model. When time increased between initial implant placement and *S. aureus* inoculation, the risk of infection decreased. All implants were highly colonised when the bacterial challenge was immediate or 1 d after implantation. 3 d following surgery there was a reduced number of bacteria on the implants. After 7 d *in situ*, the IMNs were not colonised by bacteria. These reductions in the number of colonising bacteria coincided with an increasing number of differentiated immune cells present on the implant. A protective layer of $CD45^+/CD68^+$ monocytes and macrophages was first identified on the IMN 3 d after implantation. Although at this time only half of the haematopoietic cells differentiated into macrophages and monocytes on the implant, they were able to thwart colonisation by UAMS-1GFP, the least virulent strain used in the study. The number of these immune cells increased at day 7, which allowed for almost complete thwarting of bacterial colonisation of the implants in every group. To the authors' knowledge, this is the first preclinical evidence for temporal haematopoietic differentiation directly on the surface of an orthopaedic implant with a correlating reduction in implant infection.

The stromal fraction present on the orthopaedic implant contained both non-haematopoietic ($CD45^-$) and haematopoietic ($CD45^+$) populations. Initially, a sizable proportion of the non-haematopoietic population on the implant surface co-expressed CD90, indicating many of these cells were of a spindle-cell (fibroblast or stem cell) phenotype. Throughout the course of the experiment, the

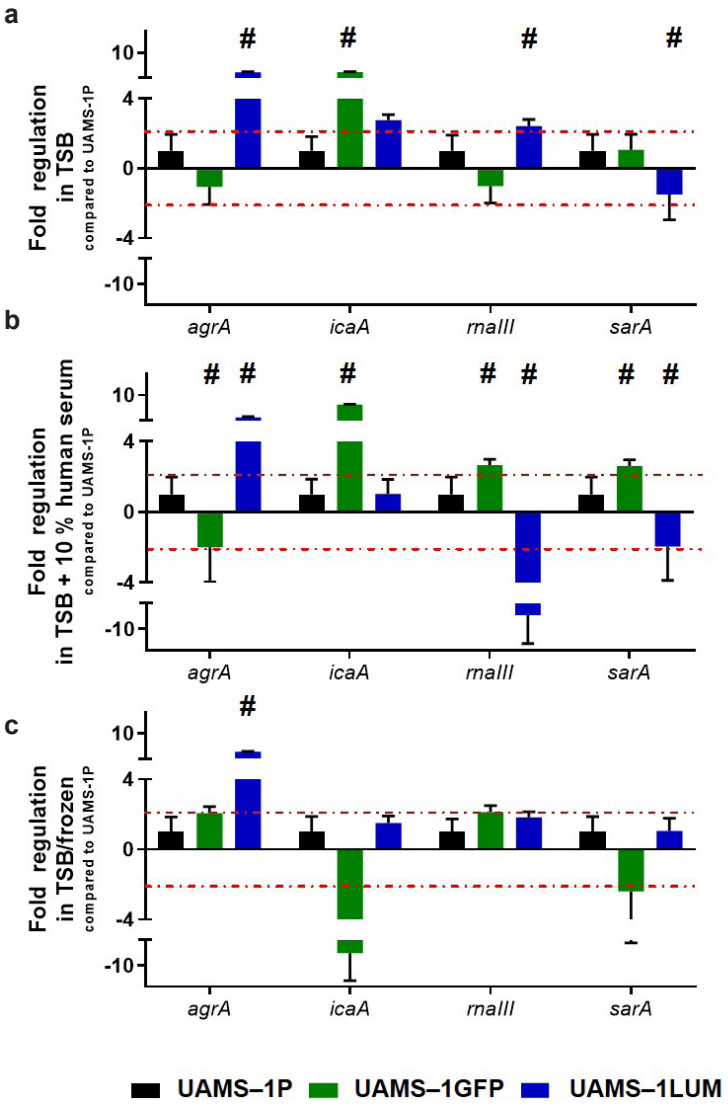

Fig. 8. Planktonic bacteria factor expression related to virulence and biofilm formation. (**a**) TSB, (**b**) TSB + 10 % human serum and (**c**) TSB then frozen. One-way ANOVA within each factor expression using Dunnett's multiple comparison to statistically compare each group to UAMS-1P. $^{\#}p < 0.05$ as compared to UAMS-1P within each preparation condition. Dotted-red line represents 2-fold biological change from UAMS-1P gene expression.

proportion of CD45⁻/CD90⁺ cells present on the IMN decreased. CD90 expression plays an important role in the maintenance of an undifferentiated state in MSCs and the loss of this cell marker on the IMN surface indicated that these cells received signals for terminal differentiation (Moraes *et al.*, 2016). While the tracking of these stem cell populations maturing into immune cells was beyond the scope of the study, Hotchkiss *et al.* (2019), using human MSCs cultured on implant surfaces, discovered an upregulation of osteoblast differentiation markers at 3 and 7 d post cell attachment. As such, it is not unreasonable to assume that the loss of CD90⁺ cell populations in the present study was due to differentiation of adherent cells. In addition to the non-haematopoietic cells, haematopoietic lineage cells were present on the surface of the implant at day 1, although this population did not co-express the monocyte/macrophage surface marker CD68 at this early time point. In contrast to the loss of CD90⁺ populations over the course of the study, the number of haematopoietic populations co-expressing the monocyte/macrophage marker CD68 drastically increased over time. This finding is supported by recent kinetic analysis of cellular colonisation on both alginate spheres and polypropylene mesh.

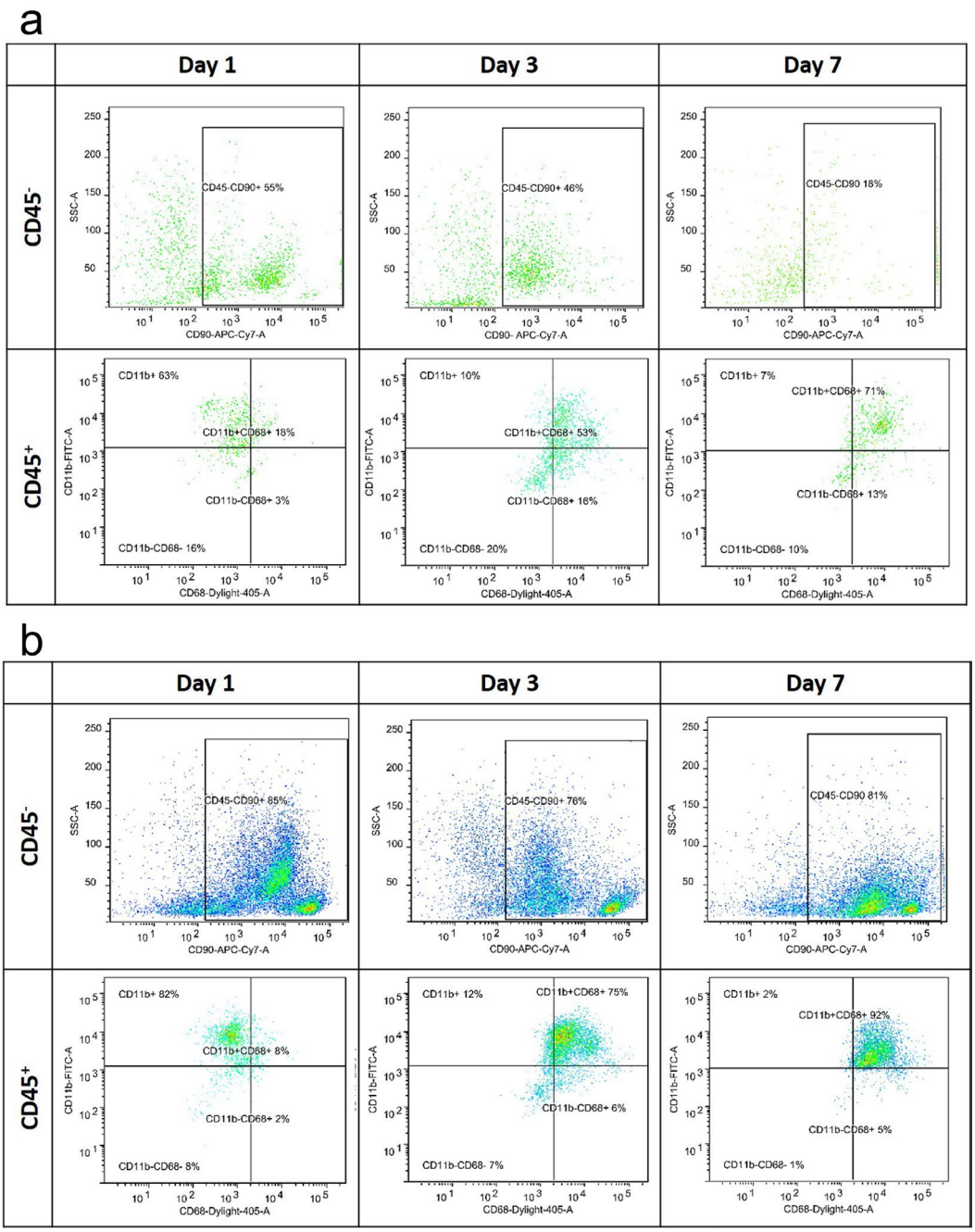

Fig. 9. Effect of time on both IMN surface adherent cells and cells found in bone marrow (BM). Flow cytometry for cells recovered from (**a**) IMN and (**b**) BM. CD45 identifies a haematopoietic cell lineage. CD11b and CD68 identify a monocytic/macrophagic lineage among CD45⁺ parent population. CD90 identifies stem cell and fibroblast cells among CD45⁻ parent population. Total populations were 25,000 cells for BM and 7,000 cells for IMN.

Table 2. Percentage of parent ($CD45^+$ or $CD45^-$) and total cell population recovered from IMN and BM after 1, 3 and 7 d *in situ*. CD45 identifies a haematopoietic cell lineage. CD11b and CD68 identify a monocytic/macrophagic lineage among $CD45^+$ parent population. CD90 identifies stem cell and fibroblast cells among $CD45^-$ parent population. Total populations were 25,00 cells for BM and 7,000 cells for IMN. Percentage total population are percentage of stained cells among total cells recovered from either IMN or BM ± SD. ND: not determined.

			Day 1		Day 3		Day 7	
Source	Parent staining	subset lineage staining	Percentage parent	Percentage total	Percentage parent	Percentage total	Percentage parent	Percentage total
BM	$CD45^+$	$CD11b^+$ $CD68^+$	15.35 ± 6.08	0.90 ± 0.51	77.71 ± 3.86	9.59 ± 1.87	57.61 ± 5.26	14.39 ± 1.93
	$CD45^-$	$CD90^+$	91.95 ± 7.54	56.79 ± 6.59	75.73 ± 11.8	34.34 ± 6.65	82.38 ± 5.25	37.60 ± 8.35
	$CD45^-$	$CD68^+$	0.02 ± 0.01	0.01 ± 0.0.1	25.16 ± 2.79	11.39 ± 1.17	18.14 ± 6.20	8.54 ± 3.79
IMN	$CD45^+$	$CD11b^+$ $CD68^+$	11.83 ± 6.66	1.97 ± 0.23	43.70 ± 8.10	10.35 ± 1.66	66.06 ± 10.47	9.8 ± 3.23
	$CD45^-$	$CD90^+$	43.60 ± 14.46	8.97 ± 2.97	11.97 ± 4.49	4.17 ± 0.91	13.33 ± 10.47	3.33 ± 2.57
	$CD45^-$	$CD68^+$	ND	ND	18.73 ± 9.72	6.66 ± 3.79	2.12 ± 1.39	0.40 ± 0.27

Veish *et al.* (2015) revealed myeloid cells ($CD11b^+$) to predominate the surface of alginate beads at day 1 and $CD68^+$ cells increasing until plateauing at 7 d post subcutaneous implantation. Similarly, polypropylene mesh induces a robust recruitment and differentiation of myeloid cells 7 d after subcutaneous implantation (Heymann *et al.*, 2019). Furthermore, the eventual accumulation of monocytic cells on titanium surfaces corroborates with previous evidence for multinucleated foreign body giant cells (FBGC) on titanium surfaces following 5-7 d in rabbit cortical bone, as multinucleated giant cells form from the fusion of macrophages (Gottlow *et al.*, 2010; Sennerby *et al.*, 1993). It should be noted that the increase in $CD68^+$ and decrease in $CD90^+$ populations in the present study were not accompanied by changes to the ratio of haematopoietic and non-haematopoietic cells within the total cell population on the implant surface. This finding indicated that cellular colonisation of the implant is an active process and that the maturing immune cell population may be present early after implantation but may require sufficient time to adopt a mature macrophage phenotype and provide protection to the implant surface. As such, alterations to cellular populations are compelling and may provide a mechanistic explanation for the reduction in bacterial colonisation of the implant seen by day 3 and 7.

It has long been known that a foreign body potentiates an infection (Elek and Conen, 1957). Implant infection likelihood, proposed by Gristina's original "race for the surface", is a widely accepted explanation for implant fate by suggesting a direct competition between host cells and bacteria to colonise the surface (Gristina, 1987; Gristina *et al.*, 1988). If the host cells integrate before the bacteria colonises it, the implant is protected, while bacterial adhesion to the implant surface is associated with an increased risk of infection. Since the introduction of the "race for the surface", multiple studies have investigated this theory. *In vitro* studies have demonstrated that the presence of bacteria or bacterial components on an implant surface greatly reduces the number of attaching osteoblastic cells and *vice versa* (Chu *et al.*, 2018; Fernández *et al.*, 2011; Lee *et al.*, 2010; Martinez-Perez *et al.*, 2017; Subbiahdoss *et al.*, 2009; Yue *et al.*, 2014), while multiple investigators have identified time as a protective factor against haematogenous infection. Using a rabbit model of hip arthroplasty and a model of subcutaneous disc implantation, these studies indicated that significant protection against bacterial contamination can be conferred by increasing the time from implantation to inoculation (Gottenbos *et al.*, 2001; Southwood *et al.*, 1985). These studies, however, did not investigate the role of host attachment to implanted materials in the likelihood of infection. While these studies provided valuable insight towards the understanding of competitive colonisation by host and bacteria, *in vitro* work does not reflect *in vivo* observations of host cell colonisation nor can it account for the role of blood components and deposition of an extracellular matrix on the implant surface. Early discoveries indicate that, rather than early colonisation by osteoblasts, the surface of a titanium implant is immediately coated with a thin layer of plasma components, followed by rapid platelet adhesion and macrophage colonisation (Sennerby *et al.*, 1993). Adherent macrophages initiate a foreign body response and undergo fusion soon after colonisation, resulting in the formation of FBGCs on the implant surface (Mariani *et al.*, 2019; Sennerby *et al.*, 1993). Similarly, subcutaneous implants elicit a foreign body immune response in a time-dependent manner, with cells of the monocyte and macrophage lineage occupying the surface and fusing to initiate the foreign body response (Higgins *et al.*, 2009). The present study confirmed that haematopoietic cells are a key player, alongside other cell types, in initial early implant integration. However, to the authors' knowledge, there is only one *in vitro* study that involves macrophages in their "race" model (Subbiahdoss *et al.*, 2011). This initial macrophage response, originally thought to impede integration and promote bacterial colonisation, is crucial for early implant protection (Anderson *et al.*, 2008; Gristina *et al.*, 1991).

The inflammatory microenvironment around an implant dictates the initiation of normal wound healing and, ideally, allows for rapid colonisation by stromal cells and appropriate immune cell populations (Anderson *et al.*, 2008). Under ideal conditions, an initial, short-lived inflammatory response protects the implant surface against bacterial colonisation while allowing for attachment and differentiation of fibroblasts and MSCs. In the present study, haematopoietic cells colonised the implant surface rapidly after implantation and quickly differentiated into immune cells of monocytic and macrophage lineage. Not only are these macrophage cells critical to initial protection of the implant against bacterial colonisation, but previous research indicates their necessity for colonisation by stem cell populations (Hotchkiss *et al.*, 2018). *In vitro* experiments indicate that macrophage polarisation does not appear to influence initial stem cell attachment; however, a predominantly pro-inflammatory macrophage phenotype may adversely affect stem cell spreading and proliferation (Wang *et al.*, 2018). While it is understood that polarisation towards a pro-inflammatory phenotype would be protective against bacterial colonisation, as this phenotype has a high phagocytic and bactericidal potential, studies have also indicated that a pro-inflammatory microenvironment may be less permissive for initiation of a FBGC response (Anderson *et al.*, 2008; Galvan-Pena and O'Neill, 2014). In the present study, it was not possible to quantify FBGCs by flow cytometry but they were identified on the IMN by histology at day 7. While the immune response varies by material and surface coating, titanium, in particular, fosters a rapid shift towards a more anti-inflammatory phenotype and, in the presence of anti-inflammatory cytokines, the rate of FBGC formation increases (Amengual-Penafiel *et al.*, 2019; Anderson *et al.*, 2008; Trindade *et al.*, 2018). The role FBGCs plays in implant protection or potential degradation is under debate (Miron and Bosshardt, 2018). Unlimited FBGC activation can lead to implant encapsulation, aseptic loosening and attraction for bacteria (Miron and Bosshardt, 2018; ten Harkel *et al.*, 2015, Mariani 2019; Trindade *et al.*, 2016). Little research has been done to characterise

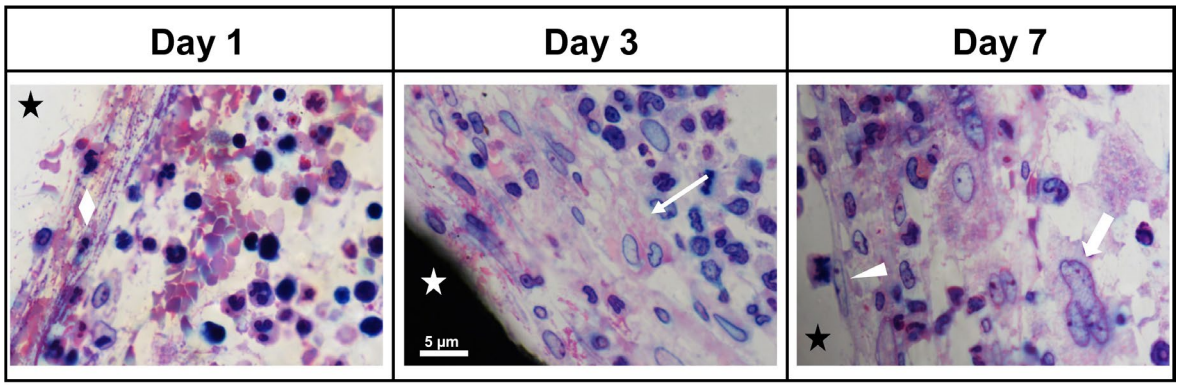

Fig. 10. Light microscopy images of the tissue adjacent to the IMN (star). Within 1 d, a thin fibrous matrix entrapping haematopoietic cells formed (diamond). After 3 d *in situ*, a thicker layer (thin arrow) of haematopoietic cells and spindle cells formed on the surface of the IMN. 7 d after implantation, multi-nucleated giant cells (arrow), other haematopoietic cells and spindle cells (arrowhead) were found near the surface of the implant. Stained with toluidine blue and basic fusion. 1,000× magnification. White part of the implant represents shrinkage artefact from tissue processing.

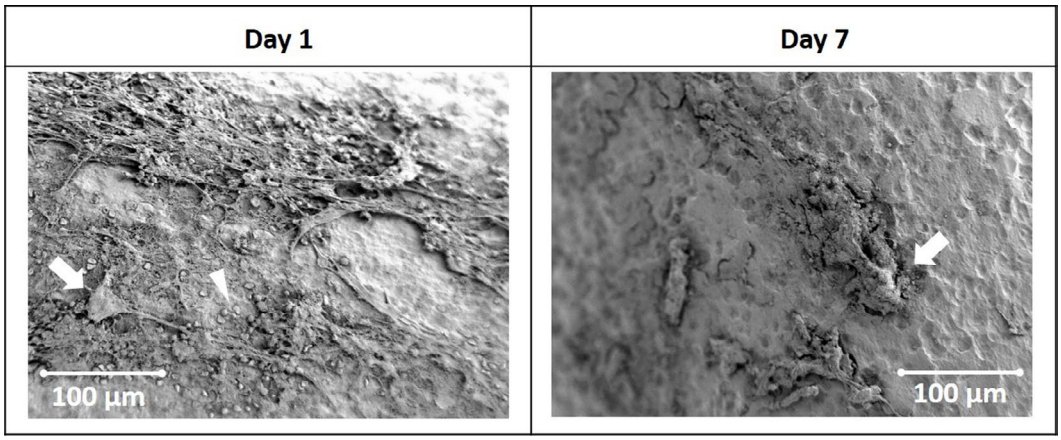

Fig. 11. SEM from day 1 and 7 showed spindle-like cells (arrow) and RBCs (arrowhead) entrapped in a matrix on the surface of the implant, when implanted for 1 d, and large macrophagic cells (arrow), when implanted for 7 d.

the specific FBGC response in the setting of bacterial infection but it is likely that, given the nature of their fusion and formation, these cells can respond to polarisation stimuli. While FBGCs generally do not represent a first line of defence against pathogen colonisation, early induction of FBGC formation and assumption of an anti-inflammatory phenotype could impede attachment of bacteria (Miron and Bosshardt, 2018). Although identifying the polarisation of the attached macrophages, subsequent FBGC formation and long-term fate of the implant was outside the scope of the study, the appropriate ratio of pro- and anti-inflammatory macrophages starts proper host attachment and promotes implant fortification (Trindade *et al.*, 2018). As such, alterations to the implant surface to promote recruitment of any specific cell type should be considered carefully in order to promote proper early cellular attachment and limit changes to the normal inflammatory environment and progression of cellular colonisation and integration (Alfarsi *et al.*, 2014).

Medical device research has focused on surface modifications to combat implant bacterial colonisation by either preventing bacterial attachment or encouraging quicker tissue integration of the implant (Campoccia *et al.*, 2013). Host-cells are more selective than bacteria: their discriminating attachment, slower motility and protracted proliferation contribute to a slower rate of integration. Modifications to the implant surface must initiate the appropriate host response while deterring a prolonged foreign body reaction that would potentiate continued dysregulation of the local immune response and prolong the implant's susceptibility to bacterial colonisation. Therefore, antimicrobial surface coatings represent a reasonable solution. There are currently two devices approved for use in high-risk patients in Europe that provide a protective surface to thwart bacterial colonisation. ImplantCast's MUTARS Silver Megaprosthesis System (implantcast GmBH, Buxtehude, Germany) uses a long-lasting silver modification to prevent bacterial attachment on surfaces not in direct contact with bone. After 28 d, roughly 30 % of the silver remains in the implant coating. Alternatively, by releasing a bolus of gentamicin within a few days of implantation, DePuy Synthes' Expert Tibial Nail PROtect hinders bacterial colonisation of the surface (Metsemakers *et al.*, 2015). These two clinical systems, used for different indications, have vastly different antimicrobial release profiles, which prompts the following questions: 1) which release profile is correct?; 2) is it dependent on anatomical location or injury type?; 3) is it dependent on the antimicrobial mechanism of action? The present study provided an understanding of the rate of bacterial colonisation of a titanium implant in the context of host cell adhesion. It gave a relevant timeline for further implant technologies seeking to reduce bacterial colonisation. By addressing the "race for the surface" in this manner, information regarding the temporal relationship between implant placement and infection susceptibility were presented. After a week *in situ*, the titanium was less prone to bacterial colonisation than groups that received a bacterial challenge immediately after surgery. This is potentially related to the significant proportion of monocytic/macrophagic host cells found on the titanium surface 7 d post-implantation. Finally, surface modifications or release of antibiotics or antimicrobials may reduce or delay the host integration with the implant, making the protective therapy less effective. This is a topic that needs to be further studied.

Importantly, the study revealed subtle differences in fluorescent and luminescent variants of *S. aureus* as compared to their UAMS-1 parental wild-type. This impacts the often-interchangeable use of reporters. Firstly, there were obvious health, weight and mortality changes when UAMS-1 was transduced with a GFP plasmid. These changes could be associated with changes in virulence caused by the transduction. For example, *Salmonella* expresses reduced pathogenic island genes and infectivity in bacteria containing the fluorescent plasmid (Knodler *et al.*, 2005). There were changes in the expression of some virulence regulators and markers of UAMS-1GFP, however, the mechanism for these virulence expression changes is unknown and beyond the scope of the present study.

The study did have limitations, as a rodent model may not directly correlate to clinical observations. Besides differences that may occur between species, anatomic location, injury severity and presence of comorbidities may also affect timeline and results. The presence of a fracture, for example, would exacerbate an infection and the inflammatory response (Morley *et al.*, 2008; Shiels *et al.*, 2018a). Both unstable fractures and fractures stabilised with implantable hardware are at increased risk of infection and, as such, further investigation of the role of fracture in the "race for the surface" is needed (Merritt and Dowd, 1987). Additionally, the present study did not investigate the role of blood supply in the rate of bacterial colonisation. It is possible that the change in blood flow to the area following IMN insertion increases the likelihood of colonisation. Schemitsch *et al.* (1994) identified a decrease in cortical blood perfusion when a sheep tibia was reamed and an intramedullary nail placed. A reamed tibia and nail placement required more time for normal blood flow to return as compared to an unreamed nail placement. Similarly, Brinker *et al.* (1999) measured 0 mL blood/min in a reamed and nailed dog tibia immediately following procedure. Within the recovery time, blood flow in the reamed tibia never returned to normal, indicating that, with the concomitant reaming and IMN placement in the present study model, blood flow was decreased to the area, therefore preventing more bacterial access. In light of this assumption, the described approach not only illustrated the interplay between host attachment and infection but also described the time line in which it occurred.

There is evidence that the types of cells that initially attach to implants remains conserved across species, from rodent to non-human primates (Hotchkiss *et al.*, 2019; Veiseh *et al.*, 2015). It is worth noting that *in vitro* cellular differentiation of both rodent and human haematopoietic precursors occurs on similar time frames, differentiating within 3 d following stimulation, as also seen in the present *in vivo* study (Alfarsi *et al.*, 2014; Gupta *et al.*, 2014; Makihira *et al.*, 2007). Additionally, the study was limited to titanium implants, one of the most common materials used for orthopaedic devices. Although different materials can cause various host responses, there is evidence that these material-based differences are lost when challenged with bacteria (Rochford, 2019). Finally, while the present study attempted to establish a temporal link between a delay in the introduction of bacteria and increased protection of an implant surface due to host colonisation, it is important to emphasise that the present model was contrived. Other means of host protection, such as deposition of fibrin or vasculature, may provide competitive inhibition for bacterial colonisation. Additionally, other means could have been used to synthesise a bacterial invasion without the use of virulent bacteria, heat-killed for example, which could provide information regarding host-cell colonisation in the presence of inflammation. However, the present study was intended to provide a potential time frame for implant protection strategies, *i.e.* antimicrobial coatings, based on an observed temporal pattern of host or bacterial colonisation and required further investigation and not intended to justify implant placement timing or the use of antimicrobials. Future investigations will allow elucidation of the changes induced to temporal patterns of colonisation in the presence of comorbidities, fractures, bacteria, bacterial components and antimicrobial agents. In summary, the dynamics of the initial colonising cells, differentiation *in situ* and time to differentiate into mature immune cells appears similar in various pre-clinical models (Sennerby *et al.*, 1993; Veiseh *et al.*, 2015). This evidence suggests that the observed time frame needed for host immunoprotection of an implant may be clinically relevant and can serve as a blueprint for material strategies for implant protection and early integration.

Conclusion

The present study not only detected a time-dependent relationship between implant surgery and bacterial colonisation, it also observed an increase in local immune populations and their diversity that was associated with a decrease in bacterial colonisation. When bacteria were inoculated after 1 week, there were little to no bacteria on the implant despite the presence of bacteria within the bone tissue. Simultaneously, over 80 % of the haematopoietic cells on the surface of the IMN had differentiated into monocytes and macrophages. This information can give guidance to investigators for development of future devices and products that can thwart bacterial attachment or hasten host integration. A relatively short-time protection may only be needed, provided that the approach does not delay or impair host adhesion.

Acknowledgements

SMS contributed to the initial concept, design, execution, collection, analysis, interpretation and final manuscript drafting. LHM contributed to design, collection, analysis, interpretation and manuscript drafting. JCW contributed to the initial concept, design, interpretation and final manuscript editing. All authors have read and approved the final submitted manuscript.

This work was partially supported by the Combat Casualty Care Research Program. The authors would like to thank the members of the Orthopaedic Trauma Department for their hard work and dedication to the project.

The views expressed in the present manuscript are those of the authors' and do not reflect the official policy or position of the U.S. Army Medical Department, Department of the Army, the DoD or the U.S. government.

References

Alfarsi MA, Hamlet SM, Ivanovski S (2014) Titanium surface hydrophilicity modulates the human macrophage inflammatory cytokine response. J Biomed Mater Res A **102**: 60-67.

Amengual-Penafiel L, Branes-Aroca M, Marchesani-Carrasco F, Jara-Sepulveda MC, Parada-Pozas L, Cartes-Velasquez R (2019) Coupling between osseointegration and mechanotransduction to maintain foreign body equilibrium in the long-term: a comprehensive overview. J Clin Med **8**. pii: E139. DOI: 10.3390/jcm8020139.

An YH, Freidman RJ (1998) Animal models in orthopaedic research. 1st Edition. CRC press. Taylor & Francis Group.

Anderson JM, Rodriguez A, Chang DT (2008) Foreign body reaction to biomaterials. Semin Immunol **20**: 86-100.

Blomgren G, Lindgren U (1981) Late hematogenous infection in total joint replacement: studies of gentamicin and bone cement in the rabbit. Clin Orthop Relat Res: 244-248.

Brinker MR, Cook SD, Dunlap JN, Christakis P, Elliott MN (1999) Early changes in nutrient artery blood flow following tibial nailing with and without reaming: a preliminary study. J Orthop Trauma **13**: 129-133.

Busscher HJ, van der Mei HC, Subbiahdoss G, Jutte PC, van den Dungen JJ, Zaat SA, Schultz MJ, Grainger

DW (2012) Biomaterial-associated infection: locating the finish line in the race for the surface. Sci Transl Med **4**: 153rv110. DOI: 10.1126/scitranslmed.3004528.

Campoccia D, Montanaro L, Arciola CR (2013) A review of the biomaterials technologies for infection-resistant surfaces. Biomaterials **34**: 8533-8554.

Chen P, Abercrombie JJ, Jeffrey NR, Leung KP (2012) An improved medium for growing Staphylococcus aureus biofilm. J Microbiol Methods **90**: 115-118.

Chu L, Yang Y, Yang S, Fan Q, Yu Z, Hu XL, James TD, He XP, Tang T (2018) Preferential colonization of osteoblasts over co-cultured bacteria on a bifunctional biomaterial surface. Front Microbiol **9**: 2219. DOI: 10.3389/fmicb.2018.02219.

Costerton JW (2005) Biofilm theory can guide the treatment of device-related orthopaedic infections. Clin Orthop Relat Res: 7-11.

Elek SD, Conen PE (1957) The virulence of *Staphylococcus* pyogenes for man; a study of the problems of wound infection. Br J Exp Pathol **38**: 573-586.

Ellington JK, Harris M, Hudson MC, Vishin S, Webb LX, Sherertz R (2006) Intracellular *Staphylococcus aureus* and antibiotic resistance: implications for treatment of staphylococcal osteomyelitis. J Orthop Res **24**: 87-93.

Fernández ICS, Busscher HJ, Metzger SW, Grainger DW, van der Mei HC (2011) Competitive time-and density-dependent adhesion of staphylococci and osteoblasts on crosslinked poly (ethylene glycol)-based polymer coatings in co-culture flow chambers. Biomaterials **32**: 979-984.

Galvan-Pena S, O'Neill LA (2014) Metabolic reprograming in macrophage polarization. Front Immunol **5**: 420. DOI: 10.3389/fimmu.2014.00420.

Gillaspy AF, Hickmon SG, Skinner RA, Thomas JR, Nelson CL, Smeltzer MS (1995) Role of the accessory gene regulator (agr) in pathogenesis of staphylococcal osteomyelitis. Infect Immun **63**: 3373-3380.

Gottenbos B, Klatter F, Van Der Mei HC, Busscher HJ, Nieuwenhuis P (2001) Late hematogenous infection of subcutaneous implants in rats. Clin Diagn Lab Immunol **8**: 980-983.

Gottfried E, Kunz-Schughart L, Weber A, Rehli M, Peuker A, Müller A, Kastenberger M, Brockhoff G, Andreesen R, Kreutz M (2008) Expression of CD68 in non-myeloid cell types. Scand J Immunol **67**: 453-463.

Gottlow J, Sennerby L, Rosengren A, Flynn M (2010) An experimental evaluation of a new craniofacial implant using the rabbit tibia model: part I. Histologic findings. Otol Neurotol **31**: 832-839.

Gristina A, Naylor P, Meador T, Myrvik Q (1991) Biomaterial surface domains: bacterial *versus* tissue cells. Interfacial Phenomena in Biological Systems. New York, Marcel Dekker Inc. pp: 105-136.

Gristina AG (1987) Biomaterial-centered infection: microbial adhesion *versus* tissue integration. Science **237**: 1588-1595.

Gristina AG, Naylor P, Myrvik Q (1988) Infections from biomaterials and implants: a race for the surface. Med Prog Technol **14**: 205-224.

Gupta D, Shah HP, Malu K, Berliner N, Gaines P (2014) Differentiation and characterization of myeloid cells. Current protocols in Immunology **104**: 22F.5.1-22F.5.28. DOI: 10.1002/0471142735.im22f05s104.

Heydorn A, Nielsen AT, Hentzer M, Sternberg C, Givskov M, Ersbøll BK, Molin S (2000) Quantification of biofilm structures by the novel computer program COMSTAT. Microbiology **146**: 2395-2407.

Heymann F, von Trotha KT, Preisinger C, Lynen-Jansen P, Roeth AA, Geiger M, Geisler LJ, Frank AK, Conze J, Luedde T, Trautwein C, Binnebosel M, Neumann UP, Tacke F (2019) Polypropylene mesh implantation for hernia repair causes myeloid cell-driven persistent inflammation. JCI Insight **4**. pii: 123862. DOI: 10.1172/jci.insight.123862.

Higgins DM, Basaraba RJ, Hohnbaum AC, Lee EJ, Grainger DW, Gonzalez-Juarrero M (2009) Localized immunosuppressive environment in the foreign body response to implanted biomaterials. The Am J Pathol **175**: 161-170.

Hotchkiss KM, Clark NM, Olivares-Navarrete R (2018) Macrophage response to hydrophilic biomaterials regulates MSC recruitment and T-helper cell populations. Biomaterials **182**: 202-215.

Hotchkiss KM, Sowers KT, Olivares-Navarrete R (2019) Novel *in vitro* comparative model of osteogenic and inflammatory cell response to dental implants. Dent Mater **35**: 176-184.

Iqbal Z, Seleem MN, Hussain HI, Huang L, Hao H, Yuan Z (2016) Comparative virulence studies and transcriptome analysis of *Staphylococcus aureus* strains isolated from animals. Scientific reports **6**: 35442. DOI: 10.1038/srep35442.

Jenkins A, Diep BA, Mai TT, Vo NH, Warrener P, Suzich J, Stover CK, Sellman BR (2015) Differential expression and roles of *Staphylococcus aureus* virulence determinants during colonization and disease. MBio **6**: e02272-02214. DOI: 10.1128/mBio.02272-14.

Kalinka J, Hachmeister M, Geraci J, Sordelli D, Hansen U, Niemann S, Oetermann S, Peters G, Löffler B, Tuchscherr L (2014) *Staphylococcus aureus* isolates from chronic osteomyelitis are characterized by high host cell invasion and intracellular adaptation, but still induce inflammation. Int J Med Microbiol **304**: 1038-1049.

Knodler LA, Bestor A, Ma C, Hansen-Wester I, Hensel M, Vallance BA, Steele-Mortimer O (2005) Cloning vectors and fluorescent proteins can significantly inhibit *Salmonella enterica* virulence in both epithelial cells and macrophages: implications for bacterial pathogenesis studies. Infect Immun **73**: 7027-7031.

Lee JH, Wang H, Kaplan JB, Lee WY (2010) Effects of *Staphylococcus epidermidis* on osteoblast cell adhesion and viability on a Ti alloy surface in a microfluidic co-culture environment. Acta Biomater **6**: 4422-4429.

Makihira S, Mine Y, Kosaka E, Nikawa H (2007) Titanium surface roughness accelerates RANKL-dependent differentiation in the osteoclast precursor cell line, RAW264.7. Dent Mater J **26**: 739-745.

Margolin W (2000) Green fluorescent protein as a reporter for macromolecular localization in bacterial cells. Methods **20**: 62-72.

Mariani E, Lisignoli G, Borzi RM, Pulsatelli L (2019) Biomaterials: foreign bodies or tuners for the immune response? Int J Mol Sci **20**. pii: E636. DOI: 10.3390/ijms20030636.

Martinez-Perez M, Perez-Jorge C, Lozano D, Portal-Nunez S, Perez-Tanoira R, Conde A, Arenas MA, Hernandez-Lopez JM, de Damborenea JJ, Gomez-Barrena E, Esbrit P, Esteban J (2017) Evaluation of bacterial adherence of clinical isolates of *Staphylococcus sp.* using a competitive model: an *in vitro* approach to the "race for the surface" theory. Bone Joint Res **6**: 315-322.

Mayberry-Carson KJ, Tober-Meyer B, Smith JK, Lambe DW Jr, Costerton JW (1984) Bacterial adherence and glycocalyx formation in osteomyelitis experimentally induced with *Staphylococcus aureus*. Infect Immun **43**: 825-833.

Merritt K, Dowd JD (1987) Role of internal fixation in infection of open fractures: studies with *Staphylococcus aureus* and *Proteus mirabilis*. J Orthop Res **5**: 23-28.

Metsemakers WJ, Reul M, Nijs S (2015) The use of gentamicin-coated nails in complex open tibia fracture and revision cases: a retrospective analysis of a single centre case series and review of the literature. Injury **46**: 2433-2437.

Miron RJ, Bosshardt DD (2018) Multinucleated giant cells: good guys or bad guys? Tissue Engineering Part B: Reviews **24**: 53-65.

Moraes DA, Sibov TT, Pavon LF, Alvim PQ, Bonadio RS, Da Silva JR, Pic-Taylor A, Toledo OA, Marti LC, Azevedo RB, Oliveira DM (2016) A reduction in CD90 (THY-1) expression results in increased differentiation of mesenchymal stromal cells. Stem Cell Res Ther **7**: 97. DOI: 10.1186/s13287-016-0359-3.

Morley J, Smith R, Pape H, MacDonald D, Trejdosiewitz L, Giannoudis P (2008) Stimulation of the local femoral inflammatory response to fracture and intramedullary reaming: a preliminary study of the source of the second hit phenomenon. J Bone Joint Surg Br **90**: 393-399.

Perez-Tanoira R, Han X, Soininen A, Aarnisalo AA, Tiainen VM, Eklund KK, Esteban J, Kinnari TJ (2017) Competitive colonization of prosthetic surfaces by *staphylococcus aureus* and human cells. J Biomed Mater Res A **105**: 62-72.

Recker M, Laabei M, Toleman MS, Reuter S, Saunderson RB, Blane B, Torok ME, Ouadi K, Stevens E, Yokoyama M, Steventon J, Thompson L, Milne G, Bayliss S, Bacon L, Peacock SJ, Massey RC (2017) Clonal differences in *Staphylococcus aureus* bacteraemia-associated mortality. Nat Microbiol **2**: 1381-1388.

Schemitsch E, Kowalski M, Swiontkowski M, Senft D (1994) Cortical bone blood flow in reamed and unreamed locked intramedullary nailing: a fractured tibia model in sheep. J Orthop Trauma **8**: 373-382.

Sennerby L, Thomsen P, Ericson L (1993) Early tissue response to titanium implants inserted in rabbit cortical bone. J Mater Sci Mater Med **4**: 240-250.

Shiels SM, Bedigrew KM, Wenke JC (2015) Development of a hematogenous implant-related infection in a rat model. BMC Musculoskelet Disord **16**: 255.

Shiels SM, Bouchard M, Wang H, Wenke JC (2018a) Chlorhexidine-releasing implant coating on intramedullary nail reduces infection in a rat model. Eur Cell Mater **35**: 178-194.

Shiels SM, Tennent DJ, Wenke JC (2018b) Topical rifampin powder for orthopedic trauma part I: Rifampin powder reduces recalcitrant infection in a delayed treatment musculoskeletal trauma model. J Orthop Res **36**: 3136-3141.

Smeltzer MS, Thomas JR, Hickmon SG, Skinner RA, Nelson CL, Griffith D, Parr TR Jr, Evans RP (1997) Characterization of a rabbit model of staphylococcal osteomyelitis. J Orthop Res **15**: 414-421.

Southward CM, Surette MG (2002) The dynamic microbe: green fluorescent protein brings bacteria to light. Mol Microbiol **45**: 1191-1196.

Southwood RT, Rice JL, McDonald PJ, Hakendorf PH, Rozenbilds MA (1985) Infection in experimental hip arthroplasties. J Bone Joint Surg Br **67**: 229-231.

Subbiahdoss G, Fernandez IC, Domingues JF, Kuijer R, van der Mei HC, Busscher HJ (2011) *In vitro* interactions between bacteria, osteoblast-like cells and macrophages in the pathogenesis of biomaterial-associated infections. PLoS One **6**: e24827. DOI: 10.1371/journal.pone.0024827.

Subbiahdoss G, Kuijer R, Grijpma DW, van der Mei HC, Busscher HJ (2009) Microbial biofilm growth *vs.* tissue integration: "the race for the surface" experimentally studied. Acta Biomater **5**: 1399-1404.

Suff N, Waddington SN (2017) The power of bioluminescence imaging in understanding host-pathogen interactions. Methods **127**: 69-78.

Sully EK, Malachowa N, Elmore BO, Alexander SM, Femling JK, Gray BM, DeLeo FR, Otto M, Cheung AL, Edwards BS (2014) Selective chemical inhibition of agr quorum sensing in *Staphylococcus aureus* promotes host defense with minimal impact on resistance. PLoS Pathog **10**: e1004174. DOI: 10.1371/journal.ppat.1004174.

ten Harkel B, Schoenmaker T, Picavet DI, Davison NL, de Vries TJ, Everts V (2015) The foreign body giant cell cannot resorb bone, but dissolves hydroxyapatite like osteoclasts. PLoS One **10**: e0139564. DOI: 10.1371/journal.pone.0139564.

Traber KE, Lee E, Benson S, Corrigan R, Cantera M, Shopsin B, Novick RP (2008) agr function in clinical *Staphylococcus aureus* isolates. Microbiology (Reading, England) **154**: 2265. DOI: 10.1099/mic.0.2007/011874-0.

Trindade R, Albrektsson T, Galli S, Prgomet Z, Tengvall P, Wennerberg A (2018) Bone immune

response to materials, part I: titanium, PEEK and copper in comparison to sham at 10 days in rabbit tibia. J Clin Med **7**. DOI: 10.3390/jcm7120526.

Trindade R, Albrektsson T, Tengvall P, Wennerberg A (2016) Foreign body reaction to biomaterials: on mechanisms for buildup and breakdown of osseointegration. Clin Implant Dent Relat Res **18**: 192-203.

Valle J, Toledo-Arana A, Berasain C, Ghigo JM, Amorena B, Penadés JR, Lasa I (2003) SarA and not sigmaB is essential for biofilm development by *Staphylococcus aureus*. Mol Microbiol **48**: 1075-1087.

Veiseh O, Doloff JC, Ma M, Vegas AJ, Tam HH, Bader AR, Li J, Langan E, Wyckoff J, Loo WS, Jhunjhunwala S, Chiu A, Siebert S, Tang K, Hollister-Lock J, Aresta-Dasilva S, Bochenek M, Mendoza-Elias J, Wang Y, Qi M, Lavin DM, Chen M, Dholakia N, Thakrar R, Lacik I, Weir GC, Oberholzer J, Greiner DL, Langer R, Anderson DG (2015) Size- and shape-dependent foreign body immune response to materials implanted in rodents and non-human primates. Nat Mater **14**: 643-651.

Verdon J, Girardin N, Lacombe C, Berjeud JM, Hechard Y (2009) δ-hemolysin, an update on a membrane-interacting pepitide. Peptides **30**: 817-823

Wang X, Wang Y, Bosshardt DD, Miron RJ, Zhang Y (2018) The role of macrophage polarization on fibroblast behavior-an *in vitro* investigation on titanium surfaces. Clin Oral Investig **22**: 847-857.

Yazdani R, Oshaghi M, Havayi A, Pishva E, Salehi R, Sadeghizadeh M, Foroohesh H (2006) Detection of icaAD gene and biofilm formation in *Staphylococcus aureus* isolates from wound infections. Iran J Public Health **35**: 25-28.

Yue C, Kuijer R, Kaper HJ, van der Mei HC, Busscher HJ (2014) Simultaneous interaction of bacteria and tissue cells with photocatalytically activated, anodized titanium surfaces. Biomaterials **35**: 2580-2587.

Zimmerli W, Sendi P (2011) Pathogenesis of implant-associated infection: the role of the host. Semin Immunopathol **33**: 295-306.

Discussion with Reviewers

David Grainger: Would the luminescence knock-in UAMS pathogenic strain exhibit higher virulence than the wild-type?
Authors: It appears that the luminescent knock-in strain exhibited higher systemic virulence than the wild-type strain. Animals performed worse, with more severe weight loss, listlessness and failure to thrive. Additionally, the luminescent strain exhibited increased *agrA* expression as compared to the wild type, a direct indicator of its virulence. Perhaps, it can be speculated that the direct insertion of the luxABCDE operon from *Photorhabus luminescens* into the *S. aureus* chromosome caused a downstream mutation resulting in increased virulence. This could potentially explain why the GFP reporter, which was inserted as a plasmid, did not increase virulence. It is interesting that a simple modification to a bacterium could have such consequences.

David Grainger: How is the "race for the surface" experimentally recapitulated in the present study if the host responded to the implant in the absence of infection?
Authors: By separating out the host response from the infection, it was possible to identify the tissue response to the implant immediately prior to when bacteria were introduced. Anthony Gristina quoted "race for the surface" as "a contest between cell integration and bacterial adhesion to the same surface…. If the race is won by tissue, then the surface is occupied and defended and is thus less available for bacterial colonization" (Gristina *et al.*, 1987). The "race for the surface" was recapitulated by investigating what cells were present on the implant at the time of bacterial inoculation to "defend" the implant surface. By introducing bacteria at different times after implant placement, the host was in the condition to have various "head starts" in this race to occupy the surface and delaying the bacterial challenge resulted in a much lower rate of infection. Assessing which cells were present at various time points after implantation of the K-wire provided insight on which cells protect the foreign body against colonisation.

Reviewer 1: For some patients receiving a fracture fixation device, the implant may sometimes be placed several days after the initial trauma (principle known as damage-control orthopaedics). Could it be that in these cases bacteria actually predate the implant in the wound, in contrast to the situation modelled in the study? Could the authors postulate how this situation may impact upon the "race for the surface" concept?
Authors: The reviewer brings up two valid topics when discussing fracture-related osteomyelitis, damage-control orthopaedics and delayed to definitive treatment. In the setting of damage-control orthopaedics, where there is preliminary stabilisation of orthopaedic injuries while more severe, life threatening injuries are attended to, one would anticipate that patients are at higher risk of orthopaedic infection. Only a few retrospective studies have investigated the rate of infection associated with damage-control orthopaedics; however, they found the prevalence of infection to be low, between 1.7 and 11 % (Harwood *et al.*, 2006; Nowotarski *et al.*, 2000; Scalea *et al.*, 2000, additional references). That being said, another study looking at war time's "outside-in" injuries reported a much higher rate of infection and attributed it to the mechanism of the injury (Mody, 2009, additional reference). Another important risk factor for infection is the time to definitive treatment. Current standard of care mandates a delay in definitive treatment until the providers have confidently cleaned and debrided unhealthy tissue. However, during this delay, one can also anticipate a surge of environmental bacteria

to contaminate the wound and increase risk of infection. Therefore, it is quite easy for the infection to pre-date the implant. For example, GA type IIIC tibial fractures, which inherently have vascular and tissue trauma, are more likely to become infected. Some of the potential reasons for this increased risk is the aetiology of the fracture, the openness to the environment and the restricted blood flow due to mangled tissues. It is prudent to assume a high risk of infection and that the infection is likely caused from the injury itself. It this case, the infection would predate the implant. If definitive treatment were administered in such a situation, it would be likely that protein and blood components would coat the implant, but host tissue and cells may exhibit delayed attachment to the implant considering its efforts would be focused on mitigating bacterial colonisation. Bacteria, on the other hand, with such a high affinity for foreign material, would readily attach and colonise the fixation device, which could lead to an infection.

Reviewer 2: Only a fraction of orthopaedic implant-related infections has the characteristics of an acute perioperative infection, showing overt clinical symptoms during the early weeks after surgery. Other infections can be classified as delayed for their late appearance, months after surgery. Do the authors think that the animal model utilised in the present work and based on bacterial enumeration 2 weeks after surgery could be predictive also for delayed infections?

Authors: Traditional classification breaks up infection timing into early, delayed and late infection. Each of these distinctions carry characteristic modalities and typical pathogens. *S. aureus* is a pathogen typical of early infections, with signs and symptoms that are apparent within 2 weeks after injury, as for the model utilised in the present study. These infections are accompanied by gross findings such as fever, inflammation, swelling and purulence. With this in mind, these early infections are only identified in a small number of elective surgeries. The sterile environment of the operating room and meticulous technique mitigates the number of opportunistic pathogens from colonising the surgical area. To adequately test the study theory while minimising the study design, higher infection rates were required and, therefore, animals were inoculated with larger numbers of bacteria than a wound would normally have been exposed to in an elective surgery. This resulted in predictable development of clinical signs of infection and allowed for collection of results in a timely manner. This being said, a previously published work by Shiels *et al.* (2015) indicated that while there is a small loss of CFU, a haematogenously derived infection with an IMN does perpetuate for at least 42 d, with indications of infection identified early just as in the present study. Therefore, this model could be used to study chronicity of infection but perhaps not late infection, where signs and symptoms can take months to appear.

Reviewer 2: *S. aureus* has progressively become known to be an intracellular pathogen, strongly attracted by host-cell surfaces and capable of efficient intracellular invasion and persistence. This is nowadays a well-established strategy for this pathogen to invade host tissues and thrive. To which extent does the classical concept of the "race to the surface" take into account this phenomenon? Can this *in vivo* study reach any conclusion concerning the role of intracellular invasion?

Authors: It is theorised that *S. aureus* infection persistence is perpetuated by either forming a complex biofilm or residing intracellularly in local cell populations, such as osteoblasts (Brady *et al.*, 2006; Wright and Nair, 2010, additional references). Although no direct evidence for this phenomenon was observed in the present study, we believe there is a constant and consistent exchange of bacteria between the two phenotypes: bacteria dispersing from a biofilm can be entrapped within host cell and bacteria released by lysed cells can attach to substrates to form a biofilm. In this manner, the "race for the surface" does not change. When host cells, such as the monocytic and macrophagic cells identified in the present study, attach, they leave very little room for bacteria, whether released from lysed cells or in interstitial spaces, to attach.

Additional References

Brady R, Leid J, Costerton J, Shirtliff M (2006) Osteomyelitis: clinical overview and mechanisms of infection persistence. Clin Microbiol Newsl **28**: 65-72.

Harwood PJ, Giannoudis PV, Probst C, Krettek C, Pape H-C (2006) The risk of local infective complications after damage control procedures for femoral shaft fracture. J Orthop Trauma **20**: 178-186.

Mody RM, Zapor M, Hartzell JD, Robben PM, Waterman P, Wood-Morris R, Trotta R, Andersen RC, Wortmann G (2009) Infectious complications of damage control orthopedics in war trauma. J Trauma Acute Care Surg **67**: 758-761.

Nowotarski PJ, Turen CH, Brumback RJ, Scarboro JM (2000) Conversion of external fixation to intramedullary nailing for fractures of the shaft of the femur in multiply injured patients. JBJS **82**: 781-788.

Scalea TM, Boswell SA, Scott JD, Mitchell KA, Kramer ME, Pollak AN (2000) External fixation as a bridge to intramedullary nailing for patients with multiple injuries and with femur fractures: damage control orthopedics. J Trauma Acute Care Surg **48:** 613-623.

Wright JA, Nair SP (2010) Interaction of staphylococci with bone. Int J Med Microbiol **300**: 193-204.

Editor's note: The Scientific Editor responsible for this paper was Fintan Moriarty.